AFRL-RY-WP-TP-2021-0153

PARAMETRIC INTERACTION OF VLF AND ELF WAVES IN THE IONOSPHERE (Preprint)

Vladimir I. Sotnikov
Multiband Multifunction Radio Frequency Sensing Branch
Multispectral Sensing & Detection Division

JUNE 2021
Final Report

AIR FORCE RESEARCH LABORATORY
SENSORS DIRECTORATE
WRIGHT-PATTERSON AIR FORCE BASE, OH 45433-7320
AIR FORCE MATERIEL COMMAND
UNITED STATES AIR FORCE

REPORT DOCUMENTATION PAGE

Form Approved
OMB No. 0704-0188

1. REPORT DATE *(DD-MM-YY)*	2. REPORT TYPE	3. DATES COVERED *(From - To)*
June 2021	Book Chapter Preprint	1 June 2021 –1 June 2021

4. TITLE AND SUBTITLE
PARAMETRIC INTERACTION OF VLF AND ELF WAVES IN THE IONOSPHERE (Preprint)

5a. CONTRACT NUMBER
N/A

5b. GRANT NUMBER

5c. PROGRAM ELEMENT NUMBER
N/A

6. AUTHOR(S)
Vladimir I. Sotnikov

5d. PROJECT NUMBER
N/A

5e. TASK NUMBER
N/A

5f. WORK UNIT NUMBER
N/A

7. PERFORMING ORGANIZATION NAME(S) AND ADDRESS(ES)
Air Force Research Laboratory
Sensors Directorate (AFRL/RYMF)
Wright-Patterson Air Force Base, OH 45433-7320
Air Force Materiel Command
United States Air Force

8. PERFORMING ORGANIZATION REPORT NUMBER

9. SPONSORING/MONITORING AGENCY NAME(S) AND ADDRESS(ES)
Air Force Research Laboratory
Sensors Directorate
Wright-Patterson Air Force Base, OH 45433-7320
Air Force Materiel Command
United States Air Force

10. SPONSORING/MONITORING AGENCY ACRONYM(S)
AFRL/RYMF

11. SPONSORING/MONITORING AGENCY REPORT NUMBER(S)
AFRL-RY-WP-TP-2021-0153

12. DISTRIBUTION/AVAILABILITY STATEMENT
DISTRIBUTION STATEMENT A. Approved for public release; distribution is unlimited.

13. SUPPLEMENTARY NOTES
PAO case number AFRL-2021-1672, Clearance Date 1 June 2021. This technical paper will be submitted as a book chapter to the forthcoming book: "Plasma Science and Technology" to be published by IntechOpen Limited. This is a work of the U.S. Government and is not subject to copyright protection in the United States. Report contains color.

14. ABSTRACT
In this Chapter we analyze a non-linear parametric interaction between Very Low Frequency (VLF) and Extremely Low Frequency (ELF) waves in the ionosphere. We demonstrate that nonlinear parametric coupling between quasielectrostatic Lower Oblique Resonance (LOR) and ELF waves significantly contributes to the VLF electromagnetic whistler wave spectrum. Analytical and numerical results are compared with experimental data obtained during active space experiments and satellite data in the plasmasphere boundary layer, where these emissions represent a distinctive subset of substorm/ storm-related VLF activity in the region devoid of substorm injected tens keV electrons and could be responsible for the alteration of the outer radiation belt boundary.

15. SUBJECT TERMS
ionospheric turbulence, plasmapause

16. SECURITY CLASSIFICATION OF:			17. LIMITATION OF ABSTRACT:	18. NUMBER OF PAGES	19a. NAME OF RESPONSIBLE PERSON (Monitor)
a. REPORT	b. ABSTRACT	c. THIS PAGE			Vladimir Sotnikov
Unclassified	Unclassified	Unclassified	SAR	24	19b. TELEPHONE NUMBER *(Include Area Code)* N/A

Parametric Interaction of VLF and ELF Waves in the Ionosphere

Vladimir I. Sotnikov

Air Force Research Laboratory, Sensors Directorate,
Wright-Patterson AFB, OH 45433, USA
vladimir.sotnikov.1@us.af.mil

Abstract

In this Chapter we analyze a non-linear parametric interaction between Very Low Frequency (VLF) and Extremely Low Frequency (ELF) waves in the ionosphere. We demonstrate that nonlinear parametric coupling between quasi-electrostatic Lower Oblique Resonance (LOR) and ELF waves significantly contributes to the VLF electromagnetic whistler wave spectrum. Analytical and numerical results are compared with experimental data obtained during active space experiments and satellite data in the plasmasphere boundary layer, where these emissions represent a distinctive subset of substorm/ storm-related VLF activity in the region devoid of substorm injected tens keV electrons and could be responsible for the alteration of the outer radiation belt boundary.

1. Introduction

The generation of VLF sideband emissions due to parametric interaction of LOR and ELF waves was first suggested in [1, 2] in an attempt to explain an experimental results observed in the ionosphere by the Aureol 3 satellite [3, 4] and during the CHARGE 2B ionospheric rocket experiment [5]. Sideband VLF wave emissions can be explained as secondary peaks above and below the primary peak. They results from parametric interaction of excited VLF and ELF waves. Next, nonlinear parametric interactions between quasi-electrostatic LOR and ELF waves

was proposed as possible generation mechanisms of VLF whistler waves in the Turbulent Plasmosphere Boundary Layer (TPBL). Excitation of these waves was analyzed through an assessment of observations from the Cluster spacecraft and Van Allen Probes [6]. To further validate a model developed in [1, 2] and adapted in [6] to explain the observations of whistler waves in the plasmasphere. In [7] a numerical solution of a system of nonlinear equations describing parametric interactions between LOR and ELF pump waves excited in the TPBL by the diamagnetic ion currents and hot ion ring instabilities [8, 9] was analyzed. Obtained results show that nonlinear coalescence of the LOR and ELF waves leads to oblique electromagnetic VLF (whistler) emissions at frequencies much greater than the LH resonance frequency, in agreement with the observations. Finally Particle-In-Cell (PIC) simulation of parametric generation of electromagnetic whistler waves will be discussed. We will start with forced linear modes in the plasma at ELF and VLF frequencies through a direct excitation of the wave electric field. The modes are forced using traveling plane waves which propagate at specific values of the wave-vector and frequency consistent with the whistler and ELF dispersion relations. We demonstrate, using a Lagrangian fluid model in the PIC code called Large Scale Plasma (LSP), that an electromagnetic ELF wave and a quasi-electrostatic VLF wave can parametrically couple to excite electromagnetic whistler waves. We also show the formation of multiple sidebands around the carrier VLF wave. This work serves to further validate a model developed in [1, 2] and adapted in [6, 7] to explain the observations of whistler waves in the plasmasphere [10].

2. VLF Waves in the Ionosphere

We analyze excitation of waves with frequencies ω several times above the lower hybrid resonance frequency, but below the one half of electron cyclotron frequency *i.e.:*

$$\omega_{LH} < \omega < \frac{1}{2}\omega_{ce} \ , \tag{1}$$

where the lower hybrid frequency ω_{LH} in the case when $\omega_{ce}^2 << \omega_{pe}^2$ is given by:

$$\omega_{LH}^2 = \frac{\omega_{pi}^2}{1+\omega_{pe}^2/\omega_{ce}^2}. \tag{2}$$

and ω_{pe} is an electron plasma frequency. Under these conditions, only one mode is excited in a cold plasma and the main features of the radiation far away from the source can be understood from the plot analogous of wave refractive index surface. This plot can be obtained using the expression for the dispersion of VLF waves:

$$\omega^2 = \frac{\omega_{LH}^2}{[1+\omega_{pe}^2/(k^2c^2)]^2}\frac{m_i}{m}\frac{k_z^2}{k^2}, \tag{3}$$

where $k^2 = k_\perp^2 + k_z^2$, k_z is the wave vector component along the magnetic field and $k_\perp$ is the perpendicular component. Figure 1 schematically plotting the wave vector component k_z against $k_\perp$ for a given ω. A great deal of the source power is radiated as quasi-electrostatic whistler waves with $\omega_{pe}^2/k^2c^2 = 1$. The real electromagnetic mode, the whistler wave, with $\omega_{pe}^2/k^2c^2 >> 1$ is radiated in oblique directions up to an angle ~ 19.5°, which is the shadow boundary determined by the long wavelength inflexion point and these waves radiate weakly compared to other portion of the spectrum.

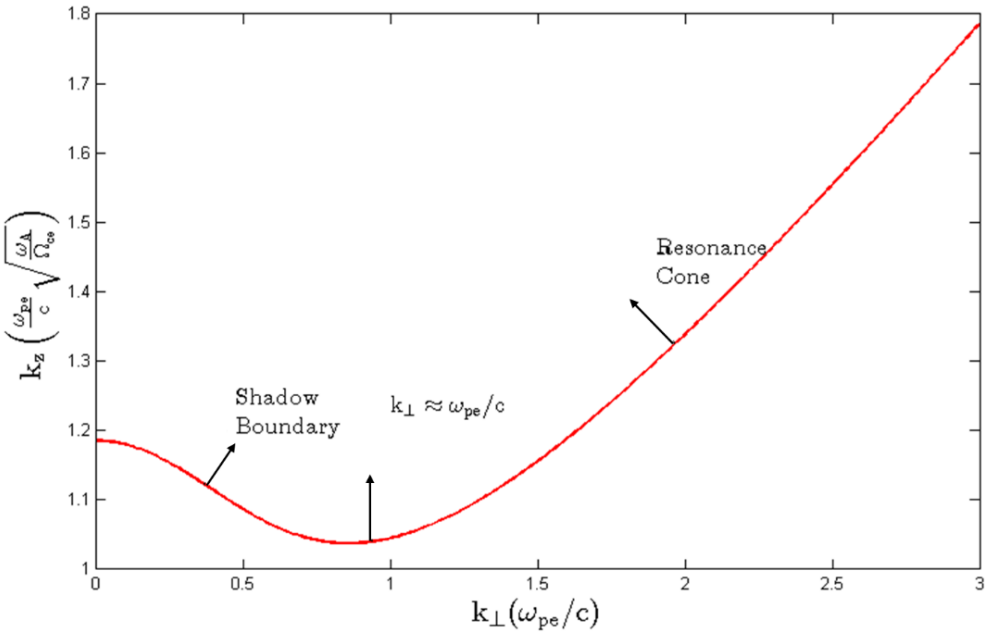

Figure 1: Wave number surface for a constant $\omega_{LH} < \omega < \frac{1}{2}\omega_{ce}$ with three critical points.

It can be shown [11], that radiation goes out in the direction of the normal to the $k_z(k_\perp)$ curve and decreases with the distance R as R^{-1} everywhere with the exception of the three critical points determining three critical directions: the two inflexion points $d^2k_z/dk_\perp^2$ where the field decreases as $R^{-5/6}$ The first inflection point corresponds to the critical angle 19.5°. The third critical point corresponds to minimum $d^2k_z/dk_\perp^2 = 0$, where the field decreases as $R^{-1/2}$, which gives the radiation along the external magnetic field.

3. Parametric Excitation of VLF Waves in the Ionosphere

Nearly monochromatic signals injected from ground-based VLF transmitters are known to experience bandwidth expansion as they traverse the ionosphere [12-16] and magnetosphere [17]. Several mechanisms have been proposed to explain this phenomenon based upon linear and nonlinear scattering assuming existence of

magnetic-field-aligned plasma density irregularities. In the absence of ionosphere irregularities a mechanism based on a parametric instability was proposed in [18-20].

Reports on sideband signals associated with VLF transmitter signals are rather scarce. Spectral peaks have been identified near the magnetic equatorial plane on the ISEE satellite at approximately ± 55 Hz of the carrier frequency (13.1 and 13.6 kHz) of Omega pulses [21]. Similar peaks seem to be observed on the COSMOS 1809 satellite and generated in the ionosphere by the carrier frequency 19 kHz [16]. Sidebands at approximately ± 500 Hz of the carrier frequency (11.9 and 12.65 kHz) of Alpha pulses have been observed in the ionosphere by the AUREOL 3 satellite [3-4].

At first sight, the 50-Hz sidebands observed on AUREOL 3 seem to correspond the Riggin and Kelly [18-1982] prediction in which the transmitted wave decays into a lower hybrid wave and an ion-acoustic type of oscillation. To account for the existence of two symmetric spectral peaks, one may replace the three-wave parametric instability considered by these authors by a four-wave parametric instability (or modulation instability) as suggested in [20]. According to this scheme, the ELF branch is due to a purely growing electrostatic mode with wave vector $\boldsymbol{k}$ large enough to provide sidebands $\pm|\mathrm{kV_s}|$ off the transmitter frequency ($\mathrm{V_s}$ is the satellite velocity). This mode is excited in course of a four-wave process by the incident VLF transmitter wave. In our case, the ELF wave branch is clearly electromagnetic and as such is of natural origin. Therefore, another explanation in accord with this experimental data has to be found.

Sotnikov et al [1] proposed another mechanism for the production of 500-Hz sidebands. It is based on nonlinear coupling between the transmitted wave and the ELF emission above the local proton gyrofrequency. The sidebands are shown to

be forced oscillations, excited only where the coupling take place. We consider the nonlinear coupling model described in the articles [1-2].

Further development of the problem of parametrically generated plasma turbulence has been developed in the articles by Sotnikov et al, [1-2] as attempt to explain appearance of symmetric sidebands emissions (secondary peaks in wave power) observed in multiple ionosphere-magnetosphere experiments, where the nonlinear coupling of the VLF transmitter signal to natural ELF emission is invoked to explain the sidebands. It was shown that the nonlinear current excited by the beats of VLF and ELF waves is strong enough to produce observed amplitude of sideband emissions. The nonlinear coupling of the VLF and ELF modes can cause a beat-wave field at the combination frequency given by

$$\omega_{\pm} = \omega_{k_1} \pm \omega_{k_2}, \tag{14}$$

which can result in sideband emissions. The sideband wave numbers are matched according to

$$k_{\pm} = k_1 \pm k_2 \tag{15}$$

Note that sidebands are not plasma eigenmodes but forced oscillations excited only where VLF to ELF wave coupling take place.

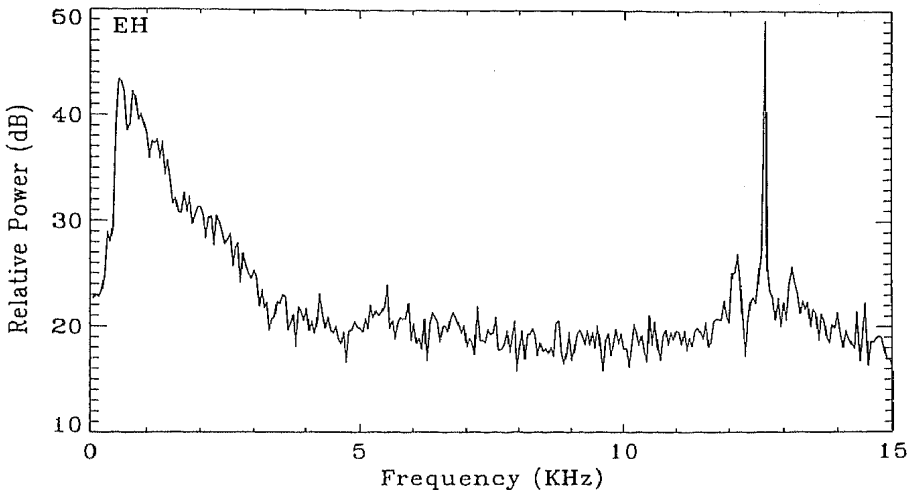

Figure 7. Averaged power spectral density of electric field. ELF natural emission at 500 Hz, VLF transmitted emission at 12.65 kHz, sidebands at frequencies (12.65 + 0.5) kHz and (12.65 - 0.5) kHz. This data were observed in ionosphere on AUREOL 3 satellite during experiments in framework of ARCAD project [3]

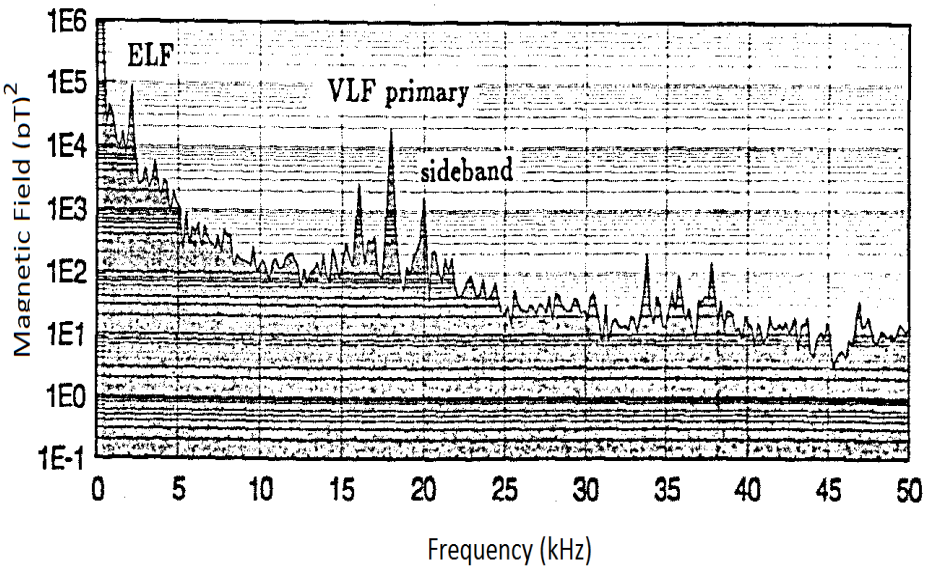

Figure 8. ELF natural emission at 2 kHz, VLF transmitted emission at 17.95 kHz, sidebands at frequencies (17.95 + 2) kHz and (17.95 - 2) kHz. This data were observed during Cooperative High-Altitude Rocket Gun Experiment (CHARGE 2B) carried out in March 1992.

Using the cold plasma approximation the equations for the perpendicular to magnetic field sideband electric field components can be derived in the form [2]:

$$E_{\perp k_+} = \frac{e}{2m}\frac{k_+}{\Omega_e \delta\omega_+}[E_{k_1} \times E_{k_2}]_z$$
$$E_{\perp k_-} = \frac{e}{2m}\frac{k_+}{\Omega_e \delta\omega_-}[E_{k_1} \times E_{k_2}]_z \quad , \qquad (16)$$

where

$$\frac{\delta\omega_{\pm}}{\Omega_e} = \frac{k_{z1}/k_1}{1+\omega_{pe}^2/(k_1^2c^2)} \pm \frac{k_{z2}/k_2}{1+\omega_{pe}^2/(k_2^2c^2)} - \frac{(k_{z1}\pm k_{z2})/k_{3\pm}}{1+\omega_{pe}^2/(k_{3\pm}^2c^2)}\ , \qquad (17)$$

$k_{3\pm}^2 = k_1^2 + k_2^2 \pm 2k_1k_2\cos(\theta)$ and θ is the angle between **k** vectors.

Sidebands may be a result of nonlinear coupling of the VLF transmitter wave and the natural ELF emission above the local proton gyrofrequency. The VLF wave propagate through the ionosphere as a whistler mode.

$$\omega_{k_1} = \Omega_e \frac{k_{1z}/k_1}{1+\omega_{pe}^2/(k_1^2c^2)} \qquad (18)$$

For the transmitted frequency $\omega/2\pi = 12$ kHZ, the corresponding wave number is $k_1 \approx 2\cdot10^{-4}$ cm^{-1}. For the known parameters whistler propagates with $\omega_{pe}^2/k_1^2c^2 = 1$ at large angle to the magnetic field.

The characteristic frequency ω_{k_2} of the ELF wave is slightly above the ion gyrofrequency and $k_2 \approx 3\cdot10^{-5}$ cm^{-1}. These waves generally propagate at large angle to the geomagnetic field. As $\omega_{pe}^2/k_2^2c^2 >> 1$, it is described by

$$\omega_{k_2} = \Omega_e \frac{k_{2z}}{k_2}\frac{k_1^2c^2}{\omega_{pe}^2}, \qquad (19)$$

where Ω_e is the electron cyclotron frequency.

4. Excitation of Whistler waves in a Turbulent Plasmapause Boundary Layer

In this section we will discuss parametric interaction of quasi-electrostatic lower oblique resonance waves excited by electron and ion diamagnetic currents and hot anisotropic ion distributions [6-9, 22-23] with ELF waves in the turbulent

plasmasphere boundary layer (TPBL). It is demonstrated below that this nonlinear mechanism can be responsible for generation of broadband, oblique Very Low Frequency (VLF) whistler (W) waves at frequencies much greater than the LH resonance frequency. It is important because the well known whistler generation mechanism by energetic electrons is unavailable in the TPB. Below we present the results of numerical solution of a system of nonlinear equations describing parametric interactions between LOR and ELF pump waves excited in the TPBL by the diamagnetic ion currents and hot ion ring instabilities [8-9]. The instabilities provide the LOR and ELF waves but do not affect nonlinear interaction. These simulation results show that nonlinear coalescence of the LOR and ELF waves leads to oblique electromagnetic VLF (whistler) emissions at frequencies much greater than the LH resonance frequency, in agreement with the observations.

In general, parametric interaction of two waves, ω_{k_1} and Ω_{k_2}, produces sidebands at the combination frequencies, $\omega_{\pm}$, that satisfy the matching conditions (14) – (15). In the case in question, we have $\omega_{\pm} \sim \omega_{k_1} >> \Omega_{k_2}$, that is, the high-frequency (VLF) and low-frequency (ELF) counterparts, with $|k_{\pm}| << |k_1| \sim |k_2|$. A general approach for solution of this problem was developed to explain symmetric sidebands, observed during active experiments with injection of a high-power VLF pump whistler wave [1] and modulated electron beam [2] into the ionosphere. It was shown that the beat waves of the VLF pump and natural ELF waves excite nonlinear currents that suffice to produce the observed VLF sidebands. That turns out to be just an initial step in the formation of a broadband VLF spectrum, because interaction of the sidebands with ELF produces secondary sidebands around the primary sidebands and so on. Thus, the relevant system of equations should be general enough to describe a broad range of

wavenumbers and frequencies. In [1-2, 6, 24] we used equations in the spectral, $\omega-\mathbf{k}$, form, just enough for estimates of the sideband amplitude. In order to describe transition to the turbulent stage, equations in time-space coordinates are required. For this particular parametric process, hydrodynamic equations of motion for magnetized electrons and unmagnetized ions are used together with Maxwell's equations. The problem is essentially three-dimensional due to the so-called vector nonlinearity [25-27] and includes two systems of equations for ELF and VLF waves interconnected through nonlinear terms. As a result of combersome but straightforward manipulations as in [1-2, 24], we can obtain nonlinear set of equations for parametric interaction of the VLF and ELF waves, which can be found in [7]. To numerically solve the resulting system of nonlinear equations and calculate the power of VLF electromagnetic emissions, a FORTRAN code was developed. The code allows studying the evolution of the electromagnetic field and electron density disturbance generated by nonlinear interaction of the VLF and ELF waves employing the predictor-corrector quasi-spectral scheme. The details of the computation can be found in [24, 28].

The elliptic-type equations are solved by spectral method using 3-D Fast Fourier Transform approach. The computational box was chosen to include 16 VLF wavelengths in the x direction, 2 ELF wavelengths in the y direction, and 1 ELF (about 4 VLF) wavelengths in the z direction. Periodic boundary conditions are applied in all directions with the grid size of 256 x 32 x 128. An initial value problem was solved with VLF and ELF pump waves turn-on all the time. The adaptive time stepping was implemented with initial dimensionless time step $\Delta\bar{t} = 2\pi\cdot 10^{-2}$ ($\Delta t \approx 10^{-5}$ s). The computation takes a few days on a standard PC. The input conditions are taken close to the observed values in the plasmasphere [22]:

$B_0 = 0.003$ G, $n_0 = 10^2$ cm^{-3}, $\omega_{ce} = 5.3\cdot 10^4$ s^{-1}, $\omega_{pe} = 5.6\cdot 10^5$ s^{-1} and $\omega_{LH} \approx 1.2\cdot 10^3$ s^{-1}.

The input VLF pump wave is a monochromatic quasi-electrostatic LOR wave at $\omega_1 \approx 5\omega_{LH}$, 3-D wavevector $k_1 = \frac{\omega_{pe}}{c}(8,0,0.94\mu^{-1/2})$, and the amplitude $E_1 = 2$ mV/m. The input ELF wave is a monochromatic MS wave with $\Omega_2 \approx 0.77\omega_{LH}$, $k_2 = \frac{\omega_{pe}}{c}(0,0.05,0.13\mu^{-1/2})$, and $E_2 = 2$ mV/m. The values of ω_1 **and** k_1, as well as Ω_2 and k_2, satisfy the dispersion equation for Fast Magnetosonic (FMS) waves :

$$\omega_k^2 = \frac{\omega_{LH}^2}{1+\frac{\omega_{pe}^2}{k^2c^2}}\left[1+\frac{M}{m}\frac{k_z^2}{k^2}\frac{1}{1+\frac{\omega_{pe}^2}{k^2c^2}}\right]$$

Note that the pump wave parameters are chosen specifically so that they are close to but not exactly satisfy the resonance conditions (equation (3)) required to get the maximal efficiency of parametric interaction, as described in [1-2]. However, in the resonance case, the collisionless system of nonlinear equations crashes after only a few time steps because of singularities that cannot be avoided, unless collisional terms are included. Figure 3 shows two-dimensional spatial spectra of the VLF pump, Φ_0 (frame a), and disturbance, $\delta\Phi$ (frames b, c, and d), taken at about 10^{-3}, 0.1, and 0.18 sec in the middle of the computational domain at y = 16, respectively. One can see that the spectral density of initially absent large-scale, $kc/\omega_{pe} << 1$, modes increases with time due to cascading toward smaller wavenumbers. As a result, the final spectrum is enriched by electromagnetic VLF waves (whistlers) at frequencies $3 < \omega/\omega_{LH} < 7.5$, with the wavenumbers indicated by rectangles (Figures 3b–3d). These waves belong to the electromagnetic part of the dispersion curves (Figure S1 in supporting information) calculated from

equation (1) with $k_\perp \approx k_x >> k_y$ (cf. the "shadow boundary" in Figure 1 in [23]). The development of oblique VLF electromagnetic emissions with the wavenumbers inside the rectangles in Figure 3 is further illustrated by Figure 4, which shows the efficiency, $\kappa_w \approx (\omega_{ce}/2\omega_w)^{1/2} E_w / E_{LH}$ as a function of time. Here E_{LH} is the root-mean-square amplitude of the total electrostatic VLF energy density outside the rectangles. The whistler wave amplitude increases with time up to the value of ~ $0.1E_1$ until the simulation is halted. This value is consistent with analytical estimate [6] and the observed VLF amplitudes. The simulation results presented in Figures 3–4 suggest the following scenario of parametric excitation of electromagnetic VLF (whistler) waves by the electrostatic VLF (LOR) and ELF pump waves. This process starts with the primary VLF sidebands, still close to the LOR branch, rapidly growing to large primary VLF sidebands, still close to the LOR branch, rapidly growing to large amplitudes of about 30% of the VLF pump amplitude. Since the parameters of the ELF pump and these sidebands

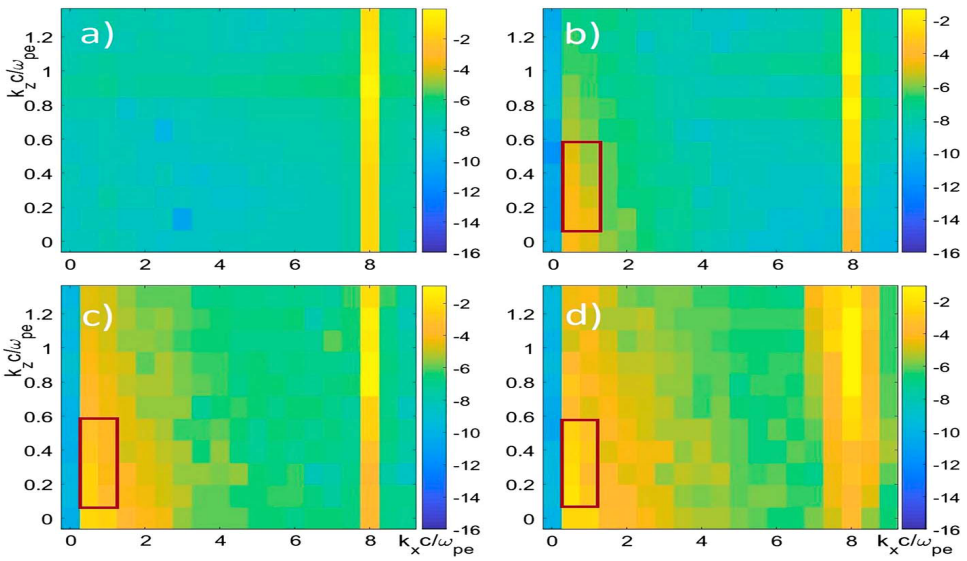

Figure 3. The 2-D Fourier spectra of the very low frequency source (a) and very low

frequency disturbance at (b) T_1, (c) $96 \cdot T_1$, and (d) $171 \cdot T_1$. The wavenumbers inside a rectangle correspond to the electromagnetic emissions at frequencies $3 < \omega / \omega_{LH} < 7.5$. Color codes in logarithmic scales are given to the right of the spectrograms. The pump waves are not "synchronized" for the resonance and this is the reason the secondary sidebands have smaller amplitudes. As a result, it takes a considerable time, relative to the growth time of the primary sidebands, to create a broad spatial and temporal VLF spectrum (Figure 3). Therefore, the electromagnetic VLF disturbance, $\delta\Phi$, increases relatively slow with time. Note that the excited ELF disturbance, $\delta\Phi$, practically does not influence the VLF emission.

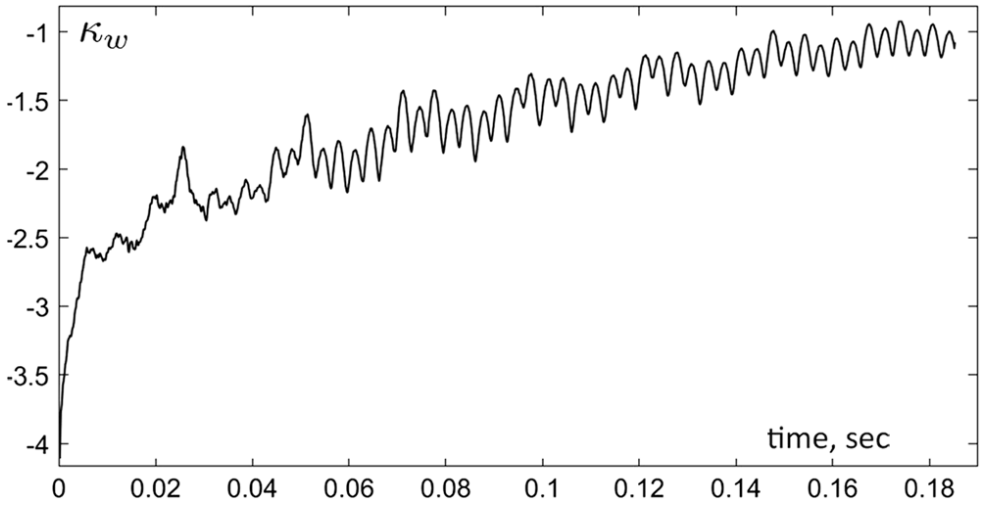

Figure 4. The whistler generation efficiency, $\kappa_w \approx (\omega_{ce} / 2\omega_w)^{1/2} E_w / E_{LH}$ in logarithmic scale versus time.

This conclusion follows from the comparison with the results of simulations with exactly the same input parameters but without taking account of the ELF

disturbance.

These waves have also been detected in the TPBL, which is devoid of substorm-injected kiloelectronvolt electrons [10, 21]. These emissions represent a distinctive subset of the substorm/storm-related VLF whistler activity and provide the rate of pitch angle diffusion of the radiation belt (RB) electrons that can explain the plasmapause-RB boundary correlation [10]. As the "standard" whistler generation mechanism by energetic electrons is unavailable in the TPBL, [6] suggested nonlinear interactions between quasi-electrostatic LH oblique resonance (LOR) and ELF waves to be the source.

Free energy for enhanced waves comes from electron diamagnetic currents in the entry layer near the TPBL's outer boundary [6,21], while diamagnetic ion currents and anisotropic (nearly ring like) hot ion distributions are the main contributors near the inner boundary [8-9]. Surprisingly, broadband, oblique Very Low Frequency (VLF) whistler (W) waves at frequencies much greater than the LH resonance frequency have also been the initial results of numerical simulations of nonlinear coupling between quasi-electrostatic lower hybrid oblique resonance and fast magnetosonic waves, which was suggested to explain the observations of Very Low Frequency (VLF) electromagnetic emissions at frequencies well above the lower hybrid resonance frequency in the TPBL. These emissions represent a distinctive subset of the substorm/storm-related VLF whistler activity contributing to the alteration of the outer radiation belt boundary. As the turbulent plasmasphere boundary layer is interior to the plasma sheet inner boundary and thus devoid of substorm-injected kiloelectronvolt electrons, the "standard" whistler generation mechanism must be excluded. Numerical results show that the parametric coupling of LOR and ELF waves creates whistler type VLF electromagnetic emissions with the spectral characteristics consistent with observations.

5. Parametric Excitation of Whistler Waves : LSP Simulation Results

A well-developed particle-in-cell plasma simulation code called Large Scale Plasma (LSP) [29] was used to perform 3D simulations of VLF field excitation. We have used the Large Scale Plasma (LSP) simulation code to force the VLF and ELF modes in a cold, magnetized plasma. We have used the Lagrangian fluid model for both the ion and the electron species. In this model, each fluid particle carries the bulk fluid velocity which is updated at each time step using the momentum equation. The fluid particles' velocity and the position are then weighted on to the grid to obtain the density and current density which supply the source terms for the field solutions. A temperature evolution equation is also solved on the grid by using the density and fluid velocity. Pressure is found on the grid from the density and temperature by assuming the plasma behaves as an ideal gas. Finally, the pressure gradient is found on the grid and weighted back to the particles (along with the fields) to update the particle velocity using the momentum equation. In addition, we use an implicit, energy conserving scheme to provide the Lorentz force push and also solve for the self-consistent electric and magnetic fields. Implicit schemes allow for larger spatial grids and time steps compared with the explicit field solvers. Because the Lagrangian scheme assumes that the plasma behaves as an ideal gas, we are assuming that the distribution function is Maxwellian. We have performed the equivalent fully kinetic simulations in 2D and obtained similar results between the fully kinetic and the Lagrangian approach. Because of the similarities, we have opted to use the Lagrangian approach. There are several advantages to using a Lagrangian fluid algorithm compared with a kinetic approach. One advantage is that the simulation particles sample fluid attributes of the plasma instead of phase space, which results in quieter simulations. A second advantage is that fewer particles per cell are needed using

the fluid model resulting in more efficient simulations. We have found good results with eight particles per cell using the fluid model compared with 200 particles per cell using a fully kinetic approach. The simulations have been performed in a 3D Cartesian geometry. The z-direction corresponds to the direction of the externally imposed magnetic field. We have assumed ionospheric parameters so that the **B**-field is set to 0.3 G and the density is 10^5 cm^{-3}. The temperature is set to 0 eV, and we have assumed hydrogen ions with a mass ratio of 1836:1. The boundary conditions are outlet boundaries which attempts to match the outgoing plasma waves in the simulation domain with a virtual wave that forms outside the simulation domain. This matching condition allows the wave to propagate out of the simulation domain and minimizes reflections back into the simulation domain. Because the plasma is cold, there is no thermal expansion of the plasma. Therefore, no particles leave the simulation domain.

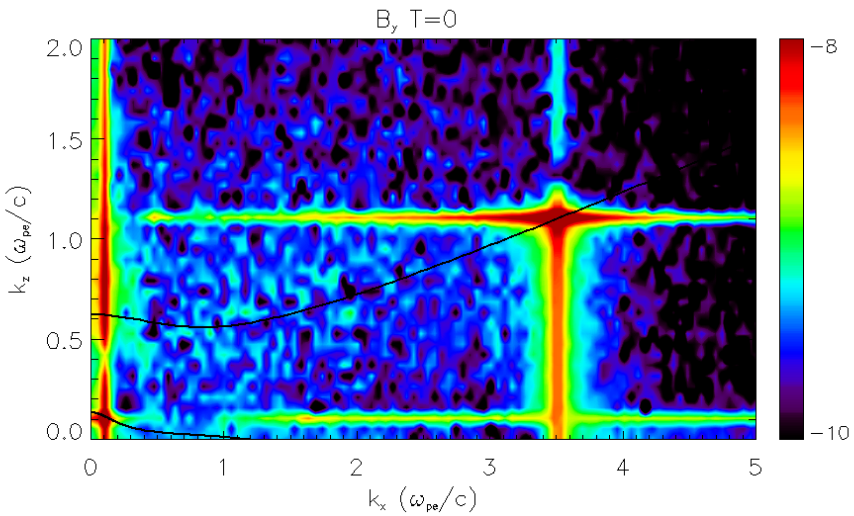

Figure 5. Power Spectra of By at t=0

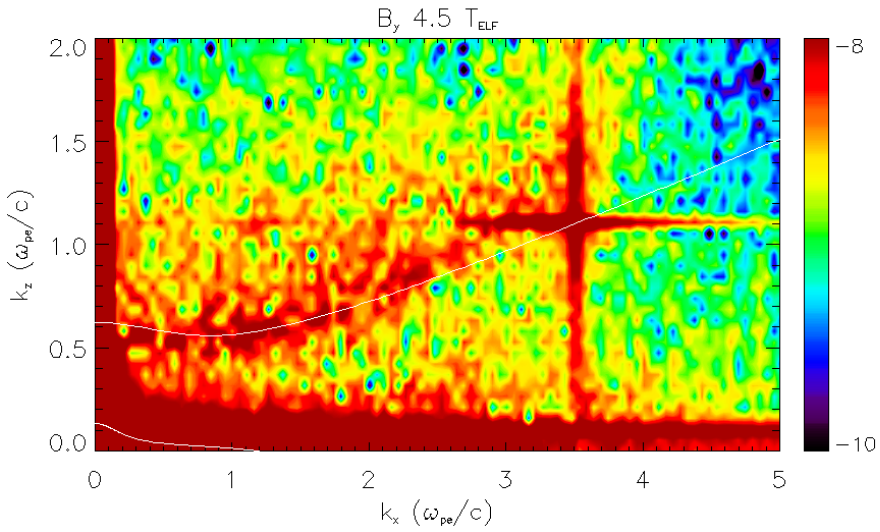

Figure 6. Power spectra of B_y at $4.5\times T_{ELF}$. Wave spectrum at a later time show excitation of modes consistent with the VLF waves dispersion presented in Figure 1 and migration of the wave spectra from a quasielectrostatic LOR to an electromagnetic whistler waves.

In LSP we can impose a traveling plane wave inside a simulation box. Both VLF and ELF waves are excited simultaneously. We choose k_x, k_y and ω. We then use the VLF and ELF dispersion to solve for k_z for these waves. Therefore, unlike the waveguide approach which excites a seemingly random set of *k*-vectors consistent with the dispersion relation, we can target any mode we desire. Because we are directly exciting specific modes, we call this method the "Direct Excitation" (DE) method. The boundary conditions are also much simpler using the DE method. We have chosen to use outlet boundaries. The waves are free to leave the simulation domain and there is little reflection of the waves at the boundaries. Finally, the simulation domain is much smaller, which allows is to make the plasma region larger and therefore resolve smaller *k*-vectors. Lastly, because we can target specific *k*-vectors, using the DE method we can test the theory and compare results from LSP with the direct solution to the equations which describe the parametric interaction. The following *k*-vectors and frequencies are used in the simulation

results shown below: $k_{VLF} = (3.5,0,1.1)\omega_{pe}/c$ and $k_{ELF} = (0.1,0.1,0.11)\omega_{pe}/c$. The ELF and VLF frequencies are $0.8\omega_{LH}$ and $12\omega_{LH}$. This set of parameters leads to $\delta\omega_+ \approx 0.013\omega_{LH}$ and $\delta\omega_- \approx 0.05\omega_{LH}$. Therefore, we expect the positive sideband to be a larger amplitude since $\delta\omega_+$ is smaller than $\delta\omega_-$ and therefore closer to resonance. Indeed, we have seen that the positive sideband is often a larger amplitude. The simulation was run for ~11 ELF periods. The VLF and ELF waves are exciting by specifying the *y*-component of the electric field only. This leads to the excitation of the other electric field components and the magnetic field. Note that we do not specifically excite B_y. Therefore all field components are excited self-consistently when only one field component is excited. The black curves in Figure 5 represent the solutions to the VLF and ELF dispersion equations. The most prominent modes occur at the wavenumbers which are driven externally. The VLF dispersion curve crosses the externally driven VLF *k*-vector and ELF dispersion crosses the externally driven ELF *k*-vector. Therefore, we are confident that we are driving the correct modes.

6. Conclusion

In this Chapter using analytical methods and PIC simulation we analyzed efficiency of excitation of electromagnetic VLF whistler waves due to parametric interaction of quasi-electrostatic LOR and ELF waves in the ionospheric plasma. $\delta\omega_{\pm} << \Omega_{k_s}$ and values of the sideband amplitudes in agreement with experimental results. It is also possible to satisfy the condition for resonance excitation of VLF waves. If we take into account resonance broadening $\Delta\omega$ due to finite collisions then $\Delta\omega \sim \frac{\omega}{\omega_{ce}}\nu$, where ν is the collision frequency. This means that for

nonresonant excitation of sidebands to occur $\delta\omega_{\pm} > \Delta\omega$ must be satisfied. In the opposite case when $\delta\omega_{\pm} < \Delta\omega$ resonant excitation mechanism takes place.

A numerical model describing nonlinear parametric coupling of LOR with ELF waves in cold collisionless plasma has been developed in order to explain the generation of VLF electromagnetic (whistler) emissions in the TPBL, which is devoid of energetic electrons. These emissions represent a distinctive subset of the substorm/storm-related VLF whistler activity interior to the plasma sheet inner boundary. The results of numerical simulations show that parametrically excited electromagnetic VLF emissions exhibit spectral features consistent with the observed VLF whistler waves.

Using PIC simulations we have directly tested the mechanism proposed in [6] by forcing a quasi-electrostatic whistler wave (i.e., a LOR wave) and an ELF mode and simulation results confirmed that this generation mechanism is feasible. Simulation results clearly show that the LOR mode has cascaded to lower wave number EM whistler modes. Therefore, the model proposed in [6] that the observed whistler waves are due to a parametric interaction between the LOR and ELF waves is consistent with the findings from the simulation results.

References

[1] Sotnikov V. I., Fiala V., Lefeuvre F., Lagoutte D., and Mogilevskii M., Excitation of sidebands due to nonlinearc ouplingb etweena VLF transmittesr signal and a natural ELF emission, J. Geophys. Res. 1991; 96, 11363-11374, DOI:10.1029 /91JA00695

[2] Sotnikov V.I., Schriver D., Ashour-Abdalla M., and Ernstmeyer J., Excitation of sideband emissions by a modulated electron beam during the CHARGE 2B mission, J. Geophys. Res. 1994; 99, 8917-8926, DOI:10.1029/93JA03024

[3] Tanaka, Y., Lagoutte, D., Hayakawa, M., Tajima, M.S., Geophys. Spectral broadening of VLF transmitter signals and sideband structure observed on Aureol 3 satellite at middle latitudes, J. Geophys. Res. 1987; 92,7551-7561

[4] Lagoutte D., Lefeuvre, F., Hanasz, J., Application of bicoherence analysis in study of wave interactions in space plasma, J. Geophys. Res. 1989; 94, 435-442

[5] Myers, N.B., and Ernstmeyer, J., Notes on the CHARGE 2B electron beam experiment platform, Tech. Memo. RL TM-92-28, Utah State University, Logan, Utah, 1992.

[6] Mishin, E.V., and Sotnikov, V.I., The turbulent plasmasphere boundary layer and the outer radiation belt boundary, Plasma Phys. Control. Fusion 2017; 59, 124003-124012

[7] Mishin E.V., Sotnikov V.I., Gershenzon N., and Amit Sharma, Whistler Waves in the Plasmasphere Boundary Layer: Nonlinear Parametric Excitation, Geophys. Res. Letters 2019; 10.1029/2019GL083432, 1-6

[8] LaBelle, J., Treumann, R.. Current-driven lower hybrid waves at the inner edge of the ring current; Journal of Geophysical Research 1988; 93, 2591–2598.

[9] Mishin, E., Burke, W., (2005). Storm time coupling of the ring current, plasmasphere and topside ionosphere: Electromagnetic and plasma disturbances, Journal of Geophysical Research 2005; 110, A07209. DOI: 10.1029/2005JA011021

[10] Mishin, E., Albert, J., & Santolik, O., SAID/SAPS-related VLF waves and the outer radiation belt boundary. Geophysical Research Letters 2011; 38, 21101-21109, DOI: 10.1029/2011GL049613

[11] Fisher R.K. and Gould R.W., Resonances cones in the field pattern of a radio frequency probe in a warm anisotropic plasma, Phys. Fluids 1971; 857-865

[12] Bell T.F., James, H.G., Inan, U.S., Katsufrakis, J.P., The apparent spectral broadening of VLF transmitter signals during transionospheric propagation. J. Geophys. Res. 1983; 88, 4813 - 4821

[13] Titova E.E., Di, V.I., Yurov, V.E., Raspopov, O.M., Trakhtengertz, V.Yu., Jiricek, T., Triska P., Interaction between VLF waves and the turbulent ionosphere. Geopys. Res. Lett. 1984, 11, 323-331

[14] Inan U.S., Bell, T.F., Spectral broadening of VLF transmitter signals observed on DE 1: A quasi-electrostatic phenomenon, J. Geophys. Res. 1985; 90, 1771-1783

[15] Tanaka, Y., Lagoutte, D., Hayakawa, M., Tajima, M.S., Spectral broadening of VLF transmitter signals and sideband structure observed on Aureol 3 satellite at middle latitudes, J. Geophys. Res. 1987; 92,7551-7562

[16] Chmyrev V.M., (1989). Parametric excitation of ELF waves and acceleration of ions during the injection of strong VLF waves into ionospher, Kosm. Issled. 1989; 27, 249-263

[17] Bell T.F. and Ngo, H.D., Electrostatic waves stimulated by coherent VLF signals propagating in and near the inner radiation belt. J. Geophys. Res. 1988; 93, 2599-261

[18] Riggin, D. and Kelley, M.C., The possible production of lower hybrid parametric instabilities by VLF ground transmitters and by natural emissions, J. Geophys. Res. 1982; 87, 2545-2553

[19] Lee M.C. and Kuo, S.P., Production of lower hybrid waves and field-aligned plasma density striations by whistlers, J. Geophys. Res. 1984; 89, 10873-10885

[20] Groves K.M., Lee, M.C., Kuo, S.P., Spectral broadening of VLF radio signals traversing the ionosphere, J. Geophys. Res. 1988; 93, 14, 683-697

[21] T. F. Bell, J. Geophys. Res. 1985; 90, 2792-2802, DOI: 10.1029/JA090iA03p02792

[22] Mishin, E., Interaction of substorm injections with the subauroral geospace: 1.Multispacecraft observations of SAID, Journal of Geophysical Research: Space Physics 2013; 118, 5782–5796, DOI: 10.1002/jgra.50548

[23] Mishin, E., Puhl-Quinn, P. A., & Santolik, O. (2010). SAID: A turbulent plasmaspheric boundary layer. Geophysical Research Letters 2010; 37, L07106, DOI: 10.1029/2010GL042929

[24] Sotnikov, V., Kim, T., Caplinger, J., Main, D., Mishin, E., Gershenzon, N., Parametric excitation of very low frequency (VLF) electromagnetic whistler waves and interaction with energetic electrons in radiation belt. Plasma Physics and Controlled Fusion 2018; 60, 7-14, DOI: 10.1088/1361-6587

[25] Ganguli, G., Rudakov, L., Scales, W., Wang, J., & Mithaiwala, Three dimensional character of whistler turbulence, Physics of Plasmas 2010; 17, 52310-52321, DOI: 10.1063/1.3420245

[26] Shapiro, V., Shevchenko, V., Solov'ev, G., Kalinin, V., Bingham, R., Sagdeev, R., Wave collapse at lower-hybrid resonance, Physics of Fluids, 1993; 5, 3148–3162.

[27] Sotnikov V., Shapiro V., Shevchenko V., Macroscopic consequences of collapse at the lower hybrid resonance. Soviet Journal of Plasma Physics 1978, 4, 252–257.

[28] Sotnikov V.I., Ivanov V.V., Presura R., Leboeuf J.N., Onishchenko O.G., Oliver B.V., Jones B., Mehlhorn T.A., Deeney C., Investigation of Compressible Electromagnetic Flute Mode Instability in Finite Beta Plasma in Support of Z-pinch and Laboratory Astrophysics Experiments, Commun. Comput. Phys. 2008; 4, 611–623

[29] Welch D.R., Rose V., Cueno M.E., Campbell, R.B. and Mehlhorn T.A., Integrated Simulation of the generation and transport of proton beams from laser-target interaction, Phys. Plasmas 2006; 14, 25-35

Acknowledgment

It is a great pleasure to thank all my collaborators and co-authors of several papers related to this topic, especially E.Mishin, N. Gershenzon, D. Main.